# Measurements of heavy-flavour decay leptons with ALICE

**Denise Moreira de Godoy on behalf the ALICE Collaboration**

SUBATECH - Ecole des Mines de Nantes, Université de Nantes, CNRS-IN2P3, Nantes, France

E-mail: moreira@subatech.in2p3.fr

**Abstract.** We present measurements of the nuclear modification factor of heavy-flavour decay leptons in p–Pb collisions at $\sqrt{s_{\rm NN}}$ = 5.02 TeV and Pb–Pb collisions at $\sqrt{s_{\rm NN}}$ = 2.76 TeV, the elliptic azimuthal anisotropy of heavy-flavour decay leptons in Pb–Pb collisions at $\sqrt{s_{\rm NN}}$ = 2.76 TeV, and the angular correlations between heavy-flavour decay electrons and charged particles in p–Pb collisions at $\sqrt{s_{\rm NN}}$ = 5.02 TeV and in pp collisions at $\sqrt{s}$ = 2.76 and 7 TeV. Results are compared to theoretical predictions.

## 1. Introduction

The ALICE experiment is dedicated to the study of the strongly-interacting medium formed in heavy-ion collisions at LHC energies. Heavy quarks, i.e. charm and beauty, are suited to access the properties of the created medium, since they are mainly produced in initial hard parton scattering processes and experience the whole evolution of the system.

The modification of the transverse momentum spectra of heavy-flavour hadrons in Pb–Pb collisions with respect to binary scaled pp collisions is sensitive to the parton energy loss within the Quark-Gluon Plasma (QGP). The measurement in p–Pb collisions is aimed at accessing cold nuclear matter (CNM) effects on heavy-flavour production, such as nuclear modification of the PDF at low $x$. The nuclear modification factors in Pb–Pb collisions ($R_{\rm AA}$) and in p–Pb collisions ($R_{\rm pPb}$) are defined as:

$$R_{\rm AA}(p_{\rm T}) = \frac{1}{\langle T_{\rm AA}\rangle}\frac{{\rm d}N_{\rm AA}/{\rm d}p_{\rm T}}{{\rm d}\sigma_{\rm pp}/{\rm d}p_{\rm T}},\ \ R_{\rm pPb}(p_{\rm T}) = \frac{1}{A}\frac{{\rm d}\sigma_{\rm pPb}/{\rm d}p_{\rm T}}{{\rm d}\sigma_{\rm pp}/{\rm d}p_{\rm T}}, \tag{1}$$

where $dN_{\rm AA}/dp_{\rm T}$ is the $p_{\rm T}$-differential yield in Pb–Pb collisions, $T_{\rm AA}$ is the nuclear overlap function in Pb–Pb collisions, which is evaluated with the Glauber model [1], $A$ is the mass number of the Pb nucleus, $d\sigma_{\rm pp}/dp_{\rm T}$ and $d\sigma_{\rm pPb/dp_T}$ are the $p_{\rm T}$-differential cross sections in pp and p–Pb collisions, respectively. For particles produced in hard-scattering processes, one expects nuclear modification factors equal to unity in absence of initial and final state effects in nuclear collisions.

The anisotropy of particle emission can be used to further investigate the QGP properties. The anisotropy is obtained from the particle azimuthal distribution in momentum space expressed as a Fourier series with respect to the reaction plane (RP), which is defined by the impact parameter direction and the beam direction [2]:

$$E\frac{{\rm d}^3N}{{\rm d}^3p} = \frac{1}{2\pi}\frac{{\rm d}^2N}{p_{\rm T}{\rm d}p_{\rm T}{\rm d}y}\left[1+2\sum_{n=1}^{\infty}v_n\cos[n(\varphi-\Psi_{RP})]\right], \tag{2}$$

where $\varphi$ is the azimuthal angle of the particle emission direction, $\Psi_{\rm RP}$ is the (true) reaction-plane angle, which is experimentally estimated from the event-plane angle. The coefficients $v_n$, which can also be

computed as $v_n = \langle \cos[n(\varphi - \Psi_{RP})] \rangle$, represent the azimuthal anisotropy magnitude of the n-th harmonic. The elliptic azimuthal anisotropy ($v_2$) of heavy-flavour hadrons at low transverse momentum provides insight into the collective motion of heavy quarks, whereas $v_2$ of heavy-flavour hadrons at high transverse momentum is sensitive to the path-length dependence of the heavy-quark energy loss within the QGP.

Another observable used to access the collective patterns in the particle production is the two-particle angular correlation, which is the differential yield of trigger-associated particle pairs in azimuth ($\Delta\varphi$) and in pseudorapidity ($\Delta\eta$):

$$C(\Delta\varphi, \Delta\eta) = \frac{1}{N_{\text{trigger}}} \frac{\mathrm{d}^2 N_{\text{pair}}}{\mathrm{d}\Delta\varphi \mathrm{d}\Delta\eta}, \tag{3}$$

where $N_{\text{trigger}}$ is the number of trigger particles and $N_{\text{pair}}$ is the number of pairs of trigger and associated particles. The angular correlation between heavy-flavour decay electrons (trigger particle) and charged particles (associated particle) in pp collisions can be used to estimate the relative contribution of beauty-hadron decay electrons to the yield of heavy-flavour decay electrons. The measurement in p–Pb collisions can be used to investigate cold nuclear matter effects and a potential existence of collective phenomena in such collisions.

In this paper, heavy-quark production is investigated by measuring electrons and muons from semi-leptonic decay channels, which have a branching ratio of the order of 10%. We present measurements of the nuclear modification factor of leptons from heavy-flavour hadron decays in p–Pb collisions at $\sqrt{s_{\text{NN}}}$ = 5.02 TeV and Pb–Pb collisions at $\sqrt{s_{\text{NN}}}$ = 2.76 TeV, the elliptic azimuthal anisotropy of heavy-flavour decay leptons in Pb–Pb collisions at $\sqrt{s_{\text{NN}}}$ = 2.76 TeV, and the angular correlations between heavy-flavour decay electrons and charged particles in pp collisions at $\sqrt{s}$ = 2.76 and 7 TeV and in p–Pb collisions at $\sqrt{s_{\text{NN}}}$ = 5.02 TeV.

## 2. ALICE experiment and particle identification

The ALICE detector is described in detail in [3]. The centrality [4] and the event-plane angle in Pb–Pb collisions are measured with the V0 detector, which comprises two scintillator counters positioned on each side of the collision vertex: V0A ($2.8 < \eta < 5.1$) and V0C ($-3.7 < \eta < -1.7$). The amplitude of the signal in the V0A detector is also used in p–Pb collisions to classify events according to the multiplicity of particles produced at backward rapidity.

Electrons are identified at mid rapidity ($|\eta| < 0.9$) with the Inner Tracking System (ITS), the Time-Projection Chamber (TPC), the Time of Flight (TOF), and the ElectroMagnetic Calorimeter (EMCal). The identification with the ITS and the TPC is based on the specific particle energy loss $\mathrm{d}E/\mathrm{d}x$ . The time of flight of particles is used to reject hadrons in the low momentum region where the hadron $\mathrm{d}E/\mathrm{d}x$ curves cross the curve corresponding to electrons measured with the TPC. The electron identification with the EMCal is based on the distribution of the energy-to-momentum $E/p$ ratio (with $E/p \approx 1$ for electrons) and the shower shape. The electron candidate sample is composed of heavy-flavour decay electrons and background electrons, which are mainly electrons from photon conversions in detector material and from Dalitz decays. The yield of background electrons is estimated using two different methods, depending on the analysis, and subtracted statistically from the identified electron sample. The first method estimates background electrons from invariant mass of electron-positron pairs, which is expected to have small values for pairs from conversions and from Dalitz decays. The second method uses a Monte Carlo (MC) calculation of the background contributions based on the measured $\pi^0$ and $\eta$-meson cross sections [5]. The selection of electrons from beauty-hadron decays is based on the track impact parameter ($d_0$), which is the distance of closest approach (DCA) between the charged track and the interaction vertex in the transverse plane. Due to the long lifetime of beauty hadrons ($c\tau \approx 500$ $\mu$m), the impact parameter of beauty-hadron decay electrons is on average larger than the one of background electrons, which also include electrons from charm-hadron decays in this case.

Muons are reconstructed with the Muon Spectrometer at forward rapidity ($-4 < \eta < -2.5$). The track candidate in the muon tracking chambers is required to be matched with the trigger chambers in order to

reject the hadronic background. A cut on $p \times \mathrm{DCA}$, where DCA is the distance between the extrapolated muon track and the interaction vertex, is applied to remove non-primary tracks. The muon candidate sample includes muons from heavy-flavour hadron decays and muons from background sources, which are mainly $\pi$ and K decays. Background muons are estimated in pp collisions via MC simulations, while the estimation in p–Pb and Pb–Pb are obtained with the measured muons from $\pi$ and K decays at mid rapidity extrapolated to forward rapidity based on MC simulations. The forward-backward asymmetry of charged particles measured by the CMS Collaboration [6] is used for the extrapolation in p–Pb analysis.

## 3. Results

For all results shown in this section, the vertical error bars represent the statistical uncertainties, the horizontal error bars indicate the bin widths and the boxes represent the total systematic uncertainties. The boxes centered at $R_{\mathrm{pPb}} = 1$ and $R_{\mathrm{AA}} = 1$ represent the normalization uncertainty. The convention used for the rapidity sign in p–Pb collisions is negative for Pb-going direction, which addresses the orientation of the muon spectrometer, and positive for p-going one.

### *3.1. Nuclear modification factors*

The pp reference for the $R_{\mathrm{AA}}$ and $R_{\mathrm{pPb}}$ measurements (Eq. 1) of electrons from heavy-flavour hadron decays at $\sqrt{s_{\mathrm{NN}}} = 2.76$ and 5.02 TeV, respectively, was obtained by using a pQCD-driven $\sqrt{s}$-scaling [7] of the measured cross section of heavy-flavour decay electrons in pp collisions at $\sqrt{s} = 7$ TeV [5] for $p_{\mathrm{T}} < 8$ GeV/$c$ and by using FONLL predictions [8] for $p_{\mathrm{T}} > 8$ GeV/$c$. The measured cross section of electrons from beauty-hadron decays in pp collisions at $\sqrt{s} = 7$ TeV [9] was scaled to 5.02 TeV and used as reference for $R_{\mathrm{pPb}}$ of electrons from beauty-hadron decays at $\sqrt{s_{\mathrm{NN}}} = 5.02$ TeV. The pp reference for the $R_{\mathrm{pPb}}$ of heavy-flavour decay muons was obtained by $\sqrt{s}$-scaling [7] of the measured cross section of muons from heavy-flavour hadron decays in pp collisions at $\sqrt{s} = 2.76$ [10] and 7 TeV [11]. The measured cross section of heavy-flavour decay muons in pp collisions at $\sqrt{s} = 2.76$ [10] was used as reference for $R_{\mathrm{AA}}$ of heavy-flavour decay muons at $\sqrt{s_{\mathrm{NN}}} = 2.76$ TeV.

Figure 1 (left panel) shows the nuclear modification factors measured for electrons from heavy-flavour hadron decays and from beauty-hadron decays in minimum bias p–Pb collisions at $\sqrt{s_{\mathrm{NN}}} = 5.02$ TeV. Results are compatible with unity within the uncertainties. The right panel of Fig. 1 shows the comparison of the measured $R_{\mathrm{pPb}}$ of electrons from heavy-flavour hadron decays to FONLL calculations [8] with EPS09 parameterization [12] for the nuclear modification of the PDFs in p–Pb collisions. The calculation describes the data within the uncertainties.

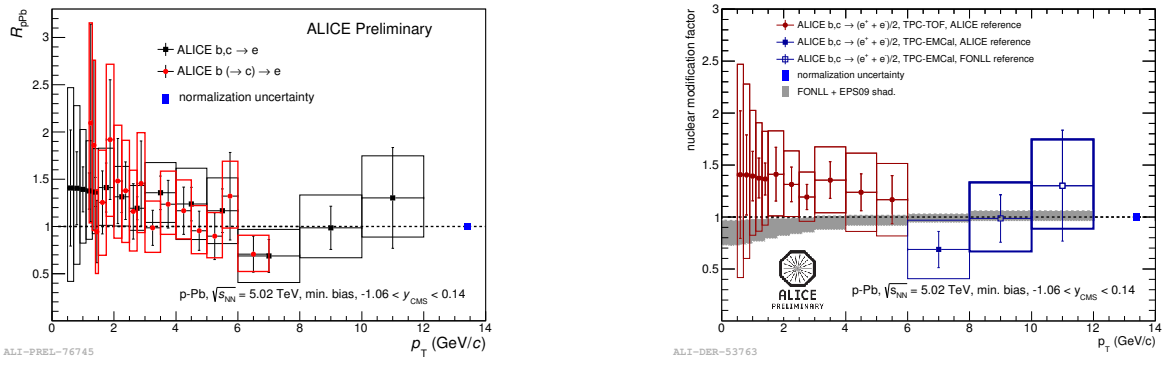


**Figure 1.** Left panel: $R_{\mathrm{pPb}}$ of electrons from decays of heavy-flavour hadrons (square symbols) and beauty hadrons (circle symbols) as a function of $p_{\mathrm{T}}$ at $\sqrt{s_{\mathrm{NN}}} = 5.02$ TeV at mid rapidity (-1.06 $< y_{CMS} <$ 0.14). Right panel: $R_{\mathrm{pPb}}$ of electrons from heavy-flavour hadron decays as a function of $p_{\mathrm{T}}$ at $\sqrt{s_{\mathrm{NN}}}$ = 5.02 TeV compared to FONLL calculations [8] with EPS09 parameterization [12] for the nuclear modification of the PDFs in p–Pb collisions.

Figure 2 shows the nuclear modification factors measured for muons from heavy-flavour hadron decays in minimum bias p–Pb collisions at $\sqrt{s_{\rm NN}}$ = 5.02 TeV at forward ($2.5 < y_{CMS} < 3.54$) and backward ($-4 < y_{CMS} < -2.96$) rapidities. Results are also compared to NLO(MNR) pQCD calculations [13] with EPS09 parametrization [12] for the nuclear modification of the PDFs in p–Pb collisions. $R_{\rm pPb}$ of heavy-flavour decay muons is compatible with unity within the uncertainties and calculations describe the data within uncertainties in different rapidities. $R_{\rm pPb}$ at low $p_{\rm T}$ in the backward rapidity region is slightly larger than unity, but consistent with the model calculation.

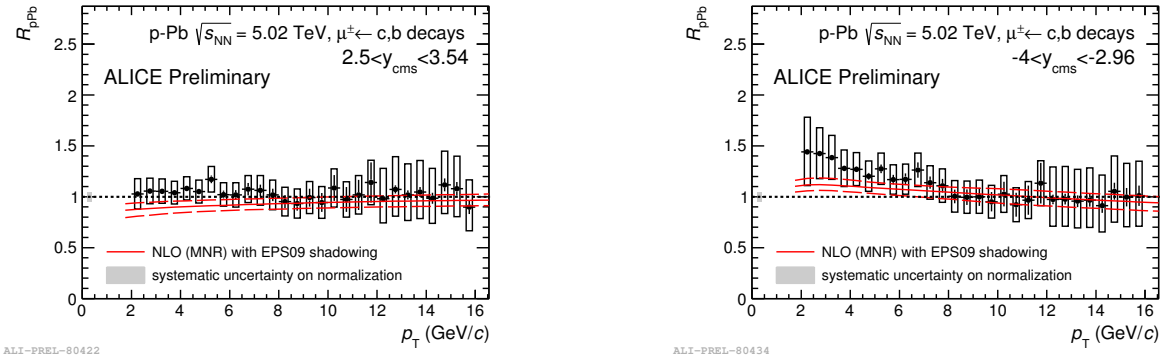


**Figure 2.** $R_{\rm pPb}$ of heavy-flavour decay muons as a function of $p_{\rm T}$ at $\sqrt{s_{\rm NN}}$ = 5.02 TeV at forward rapidity, $2.5 < y_{CMS} < 3.54$, (left panel) and backward rapidity, $-4 < y_{CMS} < -2.96$ (right panel). Results are compared to NLO(MNR) pQCD calculations [13] with EPS09 parametrization of shadowing [12].

Figure 3 (left panel) shows the nuclear modification factors ($R_{\rm AA}$) measured for electrons at mid rapidity ($|y| < 0.6$) and muons at forward rapidity ($2.5 < y < 4$), both from heavy-flavour hadron decays, as a function of $p_{\rm T}$ in Pb–Pb collisions at $\sqrt{s_{\rm NN}}$ = 2.76 TeV in the 0-10% centrality class. A strong suppression of heavy-flavour decay leptons for $p_{\rm T} > 3$ GeV/$c$ is observed in central Pb–Pb collisions. Since the measured nuclear modification factors of heavy-flavour decay leptons in p–Pb collisions are compatible with unity, this suppression suggests that heavy quarks lose energy within the created medium. Figure 3 (central panel) shows $R_{\rm AA}$ measured for electrons and muons from heavy-flavour hadron decays as a function of $p_{\rm T}$ in Pb–Pb collisions at $\sqrt{s_{\rm NN}}$ = 2.76 TeV in less central collisions (muons in the 40-80% and electrons in the 40-50% centrality class). A decrease of suppression is observed with respect to central collisions, which is consistent with the path-length dependence of the parton energy loss in the medium as well as the dependence of the medium density with the collision centrality. Figure 3 (right panel) shows $R_{\rm AA}$ measured for electrons from beauty-hadron decays at mid rapidity ($|y| < 0.8$) as a function of $p_{\rm T}$ in Pb–Pb collisions at $\sqrt{s_{\rm NN}}$ = 2.76 TeV in the 0-20% centrality class. The observed suppression of electrons from beauty-hadron decay for $p_{\rm T} > 3$ GeV/$c$ provides a hint of beauty quark in-medium energy loss.

*3.2. Elliptic azimuthal anisotropy*

The panels of Fig. 4 show the elliptic azimuthal anisotropy ($v_2$) measured for electrons at mid rapidity ($|y| < 0.7$) and muons at forward rapidity ($2.5 < y < 4$), both from heavy-flavour hadron decays, as a function of $p_{\rm T}$ in Pb–Pb collisions at $\sqrt{s_{\rm NN}}$ = 2.76 TeV for the centrality classes 0-10% (left panel), 10-20% (central panel) and 20-40% (right panel). A positive $v_2$ is observed at low $p_{\rm T}$, in particular with more than $3\sigma$ significance in the range $2 < p_{\rm T} < 3$ GeV/$c$ for heavy-flavour decay electrons and in the range $3 < p_{\rm T} < 5.5$ GeV/$c$ for heavy-flavour decay muons in the 20-40% centrality class, which indicates that charm quarks participate in the collective motion of the medium. Results suggest an increase of $v_2$ from central to semi-central collisions, which is consistent with the expectation of the evolution of the geometrical anisotropy of the overlap region of the colliding nuclei with the centrality.

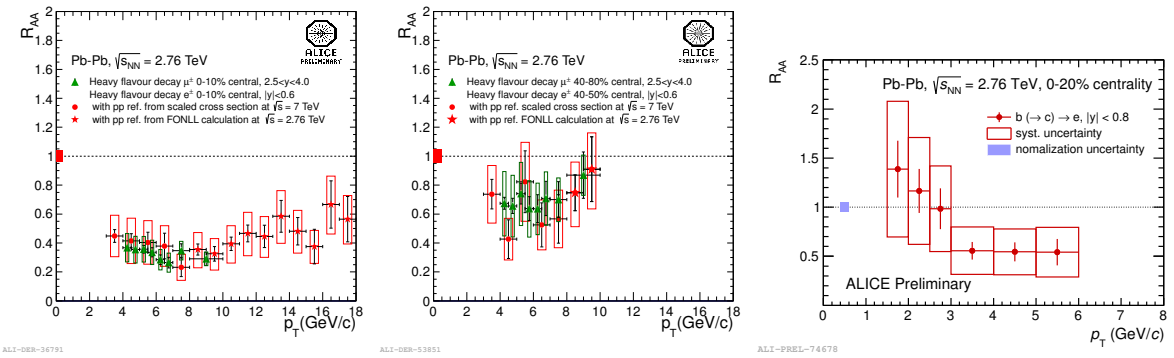


**Figure 3.** Left panel: $R_{\rm AA}$ of electrons (circle and star symbols) and muons (triangle symbols) from heavy-flavour hadron decays as a function of $p_{\rm T}$ in Pb–Pb collisions at $\sqrt{s_{\rm NN}}$ = 2.76 TeV for the centrality class 0-10%. Central panel: $R_{\rm AA}$ of electrons measured in the 40-80% and muons in the 40-50% centrality classes. For both panels, electrons are measured at mid rapidity ($|y| < 0.6$), while muons are measured at forward rapidity ($2.5 < y < 4$). Right panel: $R_{\rm AA}$ of beauty-hadron decay electrons as a function of $p_{\rm T}$ in 0-20% central Pb–Pb collisions at $\sqrt{s_{\rm NN}}$ = 2.76 TeV at mid rapidity ($|y| < 0.8$).

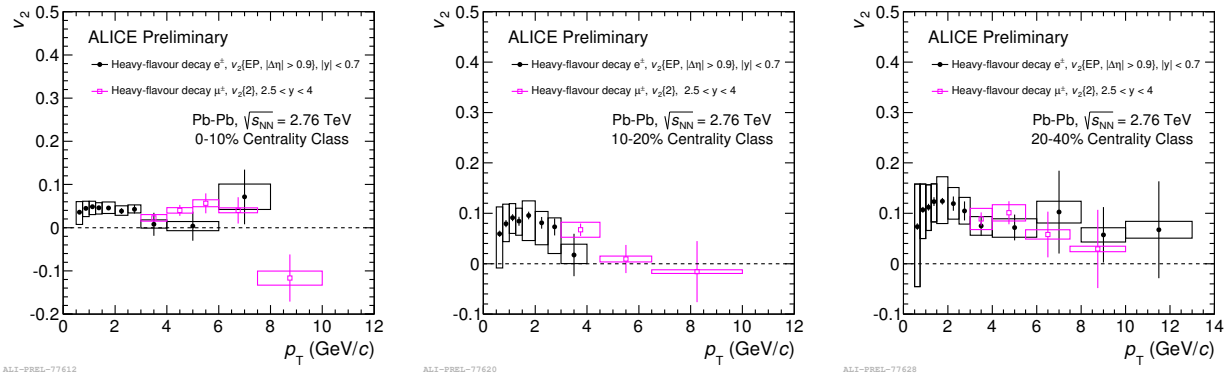


**Figure 4.** $v_2$ measured for electrons from heavy-flavour hadron decays at mid rapidity ($|y| < 0.7$) and muons from heavy-flavour hadron decays at forward rapidity ($2.5 < y < 4$) as a function of $p_{\rm T}$ in Pb–Pb collisions at $\sqrt{s_{\rm NN}}$ = 2.76 TeV in 0-10% (left panel), 10-20% (central panel) and 20-40% (right panel) centrality classes.

Figure 5 shows $v_2$ (left panel) and $R_{\rm AA}$ (right panel) of electrons from heavy-flavour hadron decays as a function of $p_{\rm T}$ measured in Pb–Pb collisions in 20-40% and 0-10% centrality classes, respectively [14]. The simultaneous comparison of $R_{\rm AA}$ and $v_2$ to model calculations [15, 16, 17, 18] presents a challenge for the latter and will eventually allow to constrain model parameters.

### *3.3. Correlations*

Figure 6 (left panel) shows the azimuthal correlation between electrons from heavy-flavour hadron decays and charged hadrons in pp collisions at $\sqrt{s}$ = 2.76 TeV at mid rapidity in two different electron $p_{\rm T}$ ranges [19]. The width of the near-side peak is larger for electrons from beauty-hadron decays than from charm-hadron decays due to the different decay kinematics of charm and beauty hadrons. The measured correlation between heavy-flavour hadron decays and charged hadrons ($e_{HF} - h$) can be expressed as a sum of the correlation between beauty-hadron decay electrons and charged hadrons ($e_b - h$) and the

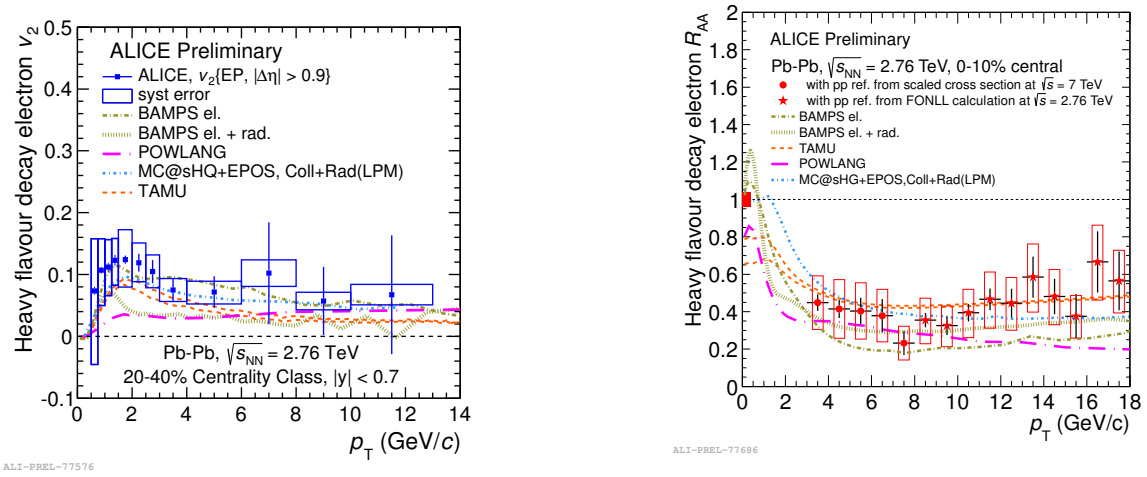


**Figure 5.** Left panel: $v_2$ of electrons from heavy-flavour hadron decays as a function of $p_{\mathrm{T}}$ measured in Pb–Pb collisions in mid rapidity ($|y| < 0.7$) in the 20-40% centrality class. Right panel: $R_{\mathrm{AA}}$ of electrons from heavy-flavour hadron decays as a function of $p_{\mathrm{T}}$ measured in 0-10% Pb–Pb collisions at mid rapidity ($|y| < 0.6$). For both panels, results are compared to parton transport models [15, 16, 17, 18].

correlation between charm-hadron decay electrons and charged hadrons ($e_c - h$):

$$C(\Delta\varphi,\Delta\eta)_{e_{HF}-h} = A + r_b C(\Delta\varphi,\Delta\eta)_{e_b-h} + (1-r_b)C(\Delta\varphi,\Delta\eta)_{e_c-h}, \tag{4}$$

where $C(\Delta\varphi,\Delta\eta)$ is defined in Eq. 3, $A$ is a constant related to the uncorrelated background, and $r_b$ is the relative contribution of electrons from beauty-hadron decays to the yield of heavy-flavour decay electrons. Equation 4 is used to fit the correlation-distribution templates obtained from a MC simulation with Pythia, for electrons from beauty and charm hadron decays separately, to the measured correlation in order to obtain the parameter $r_b$. An example of fit is shown in the left panel of Fig. 6. The right panel of Fig. 6 shows $r_b$ and the $p_{\mathrm{T}}$-differential production cross section of electrons from beauty-hadron decays in pp collisions at $\sqrt{s} = 2.76$ TeV at mid rapidity ($|y| < 0.7$) obtained via the correlation between electrons from heavy-flavour hadron decays and charged hadrons [19]. The cross section is obtained using the $r_b$ parameter and the measured heavy-flavour decay electron cross section from [20]. Results are compared to the ones obtained using the impact parameter method. The measured relative beauty contribution to the heavy-flavour decay electron yield is described by predictions from different pQCD calculations [8, 21, 22].

Figure 7 (left panel) shows the angular correlation between electrons from heavy-flavour hadron decays and charged particles at mid rapidity ($|\eta| < 0.9$) in pp collisions at $\sqrt{s}$ = 7 TeV and in p–Pb collisions at $\sqrt{s_{\mathrm{NN}}}$ =5.02 TeV for three multiplicity classes (0-20%, 20-60%, and 60-100%), which are based on V0A signal amplitude. The $p_{\mathrm{T}}$ ranges of heavy-flavour decay electrons and hadrons are 1-2 GeV/$c$ and 0.5-2 GeV/$c$, respectively. A similar shape of the angular correlation distributions is observed in low-multiplicity p–Pb collisions at $\sqrt{s_{\mathrm{NN}}}$ =5.02 TeV and in pp collisions at $\sqrt{s}$ = 7 TeV. However an increase in the yield in the near and away sides is observed in p–Pb collisions with increasing multiplicity. The observed modification can be quantified by the near side $I_{\mathrm{CP}}$, which is the ratio between the per-trigger yield in high and low multiplicity collisions:

$$I_{\mathrm{CP}} = \frac{\mathrm{yield}(-\pi/2 < \Delta\varphi < \pi/2)_{0\%-20\%}}{\mathrm{yield}(-\pi/2 < \Delta\varphi < \pi/2)_{60\%-100\%}}. \tag{5}$$

The measured near side $I_{\mathrm{CP}}$ in p–Pb collisions at $\sqrt{s_{\mathrm{NN}}}$ =5.02 TeV as a function of electron $p_{\mathrm{T}}$ (central panel of Fig. 7) indicates that there is an enhancement of associated particles for low-$p_{\mathrm{T}}$ electrons in

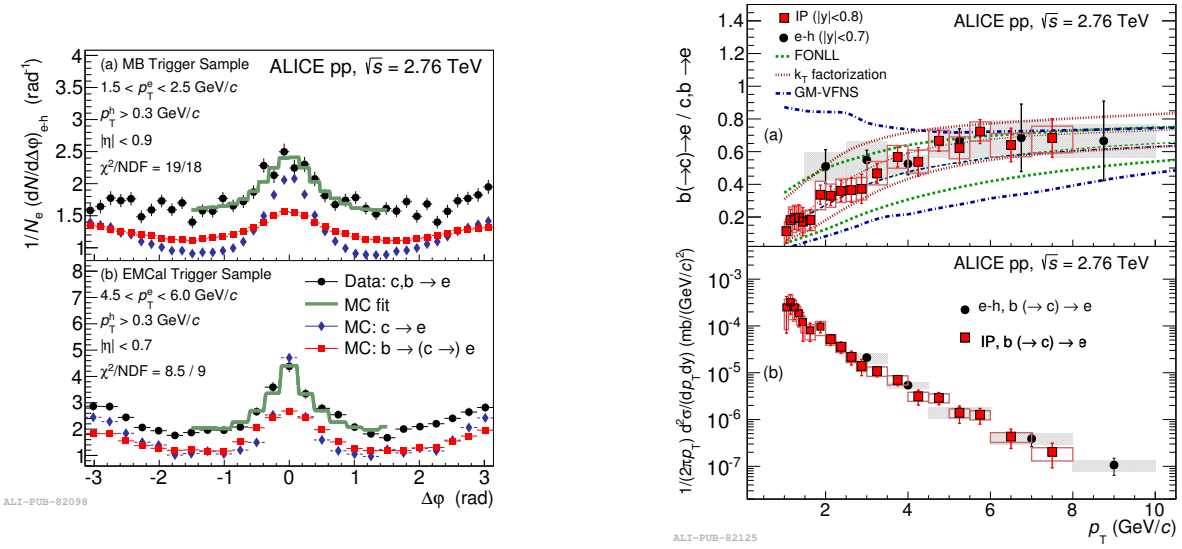


**Figure 6.** Left panel: azimuthal correlation between electrons from heavy-flavour hadron decays and charged hadrons in pp collisions at $\sqrt{s}$ = 2.76 TeV (a) low-$p_{\mathrm{T}}$ electrons ($1.5 < p_{\mathrm{T}}^{e} < 2.5$ GeV/$c$) are measured in the MB trigger sample for $|\eta| < 0.9$ (b) high-$p_{\mathrm{T}}$ electrons ($4.5 < p_{\mathrm{T}}^{e} < 6$ GeV/$c$) are measured in the EMCal trigger sample for $|\eta| < 0.7$. The circles indicate the data points, the diamond symbols represent the MC distribution for charm-hadron decay electrons, square symbols are the MC distribution for beauty-hadron decay electrons, and the line represents the MC fit (Eq. 4). Right panel: (a) relative contribution of electrons from beauty-hadron decays to the heavy-flavour decay electron yield. Results are compared to different pQCD calculations [8, 21, 22]. (b) $p_{\mathrm{T}}$-differential inclusive production cross section of electrons from beauty-hadron decays. The circle symbols represent the data points measured via the azimuthal correlation between electrons from heavy-flavour hadron decays and charged hadrons, and the square symbols are the data points obtained using the impact parameter method.

high-multiplicity p–Pb collisions. The enhancement observed for heavy-flavour decay electrons with $1 < p_{\mathrm{T}} < 2$ GeV/$c$ is further investigated by subtracting the measured correlation in $\Delta\varphi$ and $\Delta\eta$ in low multiplicity (60-100%) collisions from the one measured in high multiplicity (0-20%) events, in order to remove the contribution from jets. The result shown in Fig. 7 (right panel) indicates a long-range correlation in $\Delta\eta$, also observed for light-flavour hadron-hadron angular correlations measured in p–Pb collisions at $\sqrt{s_{\mathrm{NN}}}$ = 5.02 TeV [23, 24]. For light-flavour hadrons, this double-ridge structure can be described by calculations including gluon saturation in the initial state [25] and by models assuming an hydrodynamic expansion of final state particles in small systems [26, 27].

## 4. Conclusions

The $p_{\mathrm{T}}$-differential production cross section of electrons from beauty-hadron decays and the relative contributions of electrons from beauty-hadron decays to the yield of heavy-flavour decay electrons are obtained in pp collisions at $\sqrt{s}$ = 2.76 TeV using two different techniques, which agree with each other within the uncertainties. Measurements of $R_{\mathrm{pPb}}$ of electrons from heavy-flavour hadron decays and from beauty-hadron decays at mid rapidity and $R_{\mathrm{pPb}}$ of heavy-flavour decay muons at forward and backward rapidities are compatible with unity. A double-ridge structure is observed in the correlation between heavy-flavour decay electrons and charged particles in p–Pb collisions at $\sqrt{s_{\mathrm{NN}}}$ = 5.02 TeV. A similar structure is also observed in light-flavour hadron-hadron correlations, where it can be described by either initial or final state effects. The investigation of the double-ridge structure in heavy-flavour hadron decays, whose statistics will be significantly increased in Run 2, can contribute to clarify the origin of

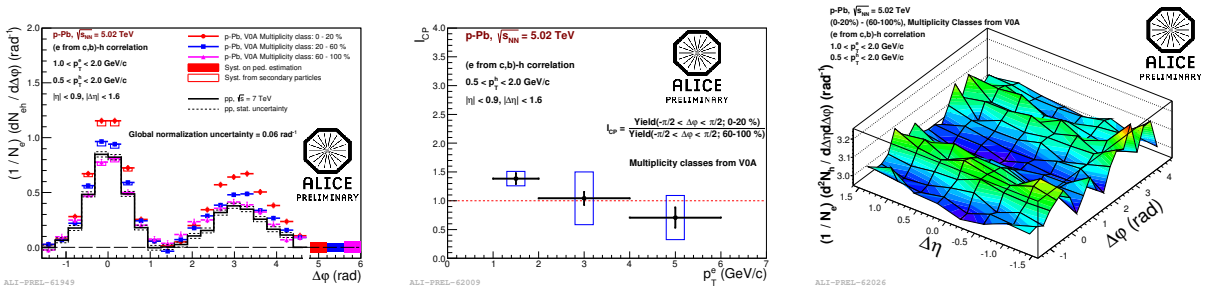


**Figure 7.** Left panel: azimuthal correlation between low-$p_{\mathrm{T}}$ electrons ($1 < p_{\mathrm{T}}^{e} < 2$ GeV/$c$) from heavy-flavour hadron decays and low-$p_{\mathrm{T}}$ charged hadrons ($0.5 < p_{\mathrm{T}}^{h} < 2$ GeV/$c$) at mid rapidity ($|\eta| < 0.9$, $|\Delta\eta| < 1.6$). The histogram represents the measument in pp collisions at $\sqrt{s}$ = 7 TeV. The circles, squares and triangles represent the measurement in p–Pb collisions at $\sqrt{s_{\mathrm{NN}}}$ = 5.02 TeV in the 0-20%, 20-60% and 60-100% multiplicity classes, respectively. Central panel: ratio between the near-side yields in high (0-20%) and low (60-100%) multiplicity classes (Eq. 5) as a function of electron $p_{\mathrm{T}}$ in p–Pb collisions at $\sqrt{s_{\mathrm{NN}}}$ = 5.02 TeV at mid rapidity ($|\eta| < 0.9$, $|\Delta\eta| < 1.6$). Right panel: Difference between the two-particle correlation distributions in $\Delta\varphi$ and in $\Delta\eta$ measured in high (0-20%) and low (60-100%) multiplicity classes in p–Pb collisions at $\sqrt{s_{\mathrm{NN}}}$ = 5.02 TeV at mid rapidity ($|\eta| < 0.9$, $|\Delta\eta| < 1.6$).

the effect. Measurements of $R_{\mathrm{AA}}$ of heavy-flavour decay leptons in central Pb–Pb collisions at $\sqrt{s_{\mathrm{NN}}}$ = 2.76 TeV show a strong suppression of heavy-flavour decay leptons at intermediate and high $p_{\mathrm{T}}$. Results of $R_{\mathrm{pPb}}$ and $R_{\mathrm{AA}}$ of heavy-flavour decay leptons suggest small cold nuclear matter effects and indicate that the suppression observed in Pb–Pb collisions is due to the presence of the hot and dense medium. The measurement of the $R_{\mathrm{AA}}$ of beauty-hadron decay electrons in the 20% most central Pb–Pb collisions hints at a suppression for $p_{\mathrm{T}} > 3$ GeV/$c$, which could indicate in-medium energy loss of beauty quarks. A positive $v_2$ of electrons and muons from heavy-flavour hadron decays is observed with more than 3$\sigma$ significance in Pb–Pb collisions at $\sqrt{s_{\mathrm{NN}}}$ = 2.76 TeV in the 20-40% centrality class, which suggests collective motion of low-$p_{\mathrm{T}}$ charm quarks.

## References


[1] M. L. Miller, K. Reygers, S. J. Sanders and P. Steinberg, Ann. Rev. Nucl. Part. Sci. 57, 205 (2007).
[2] A. M. Poskanzer and S. A. Voloshin, Phys. Rev. C 58 (1998) 1671–1678.
[3] ALICE Collaboration, JINST 3 (2008) S08002.
[4] ALICE Collaboration, Phys. Rev. Lett. 106 (2011) 032301.
[5] ALICE Collaboration, Phys. Rev. D 86 (2012) 112007.
[6] CMS Collaboration, CMS-PAS-HIN-12-017.
[7] R. Averbeck, N. Bastid, Z. Conesa del Valle, P. Crochet, A. Dainese, X. Zhang, arXiv:1107.3243 [hep-ph] (2011).
[8] M. Cacciari, M. Greco and P. Nason, JHEP 9805 (1998) 7 ; M. Cacciari, S. Frixione and P. Nason, JHEP 0103 (2001) 6.
[9] ALICE Collaboration, Physics Letters B 721 (2013) 13–23.
[10] ALICE Collaboration, Phys. Rev. Lett. 109 (2012) 112301.
[11] ALICE Collaboration, Physics Letters B 708 (2012) 265–275.
[12] K.J. Eskola, H. Paukkunen, and C.A. Salgado, JHEP04 2009 (2009).
[13] M. Mangano, P. Nason, G. Ridolfi, Nuclear Physics B 373 (1992) 295–345.
[14] Z. C. del Valle for the ALICE Collaboration, Nuclear Physics A 904–905 (2013) 178c–185c.
[15] J. Uphoff, O. Fochler, Z. Xu and C. Greiner, Physics Letters B 717 (2012) 430–435.
[16] M. He, R. J. Fries and R. Rapp, arXiv:1208.0256 [nucl-th] (2012).
[17] M. Monteno, W. M. Alberico, A. Beraudo, A. De Pace, A. Molinari, M. Nardi and F Prino, J. Phys. G. 38 (2011) 124144.
[18] P. B. Gossiaux, R. Bierkandt and J. Aichelin, Phys. Rev. C 79 (2009) 044906.
[19] ALICE Collaboration, arXiv:1405.4144 [nucl-ex] (2014).
[20] ALICE Collaboration, arXiv:1405.4117 [nucl-ex] (2014).
[21] P. Bolzoni, G. Kramer, Nucl.Phys. B 872 (2013) 253.
[22] R. Maciula, A. Szczurek, Phys.Rev. D 87 9 (2013) 094022.

[23] ALICE Collaboration, Phys.Lett. B 719 (2013) 29–41.
[24] ALICE Collaboration, Phys.Lett. B 726 (2013) 164–177.
[25] K. Dusling and R. Venugopalan, Phys. Rev. D 87 (2013) 094034.
[26] K. Werner , I. Karpenko and T. Pierog, Phys. Rev. Lett. 106 (2011) 122004.
[27] P. Bozek and W. Broniowski, arXiv:1403.6042 (2014).